CDF/ANAL/TOP/CDFR/6360

A Study of W Boson Mass Reconstruction and Top Quark Event Tagging as a Function of Jet Cluster Cone Size

Wojciech Fedorko, Pierre Savard and Pekka K. Sinervo
University of Toronto

5 March 2003

Abstract

We report a Monte Carlo study of the effect of jet clustering cone size and transverse momentum cuts on the dijet mass resolution and the event selection efficiency on top quark pair production in the CDF II detector. We find that a cone size $R = 0.35$ maximizes the reconstruction efficiency for $W+ \geq 4$ jet events, whereas larger cone sizes only tend to improve the dijet mass resolution. These results suggest a strategy that employs different definitions of jets in identifying $t\bar{t}$ events and extracting mass information from them.

1 Introduction

The aim of this study is to identify the effects that degrade W mass resolution in $t\bar{t}$ events, evaluate the importance of those effects and suggest possible solutions. We also explore the effect of the JETCLU cone size parameter, R, on the W mass resolution, and how this parameter could be optimized taking into account the varying jet-to parton matching efficiency.

Earlier studies of the jet clustering and event reconstruction in general [1] have attempted to characterize the event yield and/or the mass resolution obtained from reconstructed jets. It is well-known that with the CDF Run I $t\bar{t}$ mass reconstruction algorithm, only about 40-50% of all $t\bar{t}$ events were properly reconstructed, with the rest of the events suffering some form of misreconstruction due to incorrect parton assignments to the four leading jets in the event [2]. In this study, we explicitly have decided to avoid looking at the resolution effects due to parton misassignment, and have instead focussed on two, largely separable issues:

1. the probability of reconstructing correctly the jet from a given parton for a given cone size, and

2. the dijet mass resolution for the $W \rightarrow q\bar{q}'$ final state, in those cases where the jet-parton assignments for the W boson daughters are correct.

In order to draw conclusions, we consider three largely independent figures of merit in determining what is the most effective jet-clustering algorithm: i) the rate at which the W daughter system is correctly reconstructed, ii) the rate at which the 4 jets from the $t\bar{t}$ decay are correctly reconstructed, and iii) the mass resolution of the dijet system produced in the hadronic W decay. We believe that these three criteria provide a subset of the basic criteria that should be used to assess the performance of any parton-jet reconstruction technique.

2 Procedure

2.1 MC generation and simulation

We generated samples of $t\bar{t}$ decays using the HERWIG Monte Carlo generator (we used version 6.202 -cdfsoft v.4.6.2) [3]. Each sample was filtered at the generator level: We require that in each event one W decays hadronically and the other decays leptonically. In addition we remove events where the leptonic decay of the W produces a τ lepton. This is done so that the selected events maximally resemble the real events we would like to accept through any given lepton+jets channel. After this filter has been applied, we are left with about 100K events remaining from a generated sample of about 340K. We then perform the detector simulation with vertex smearing turned off and subsequently run the JetCluModule on these events, with a given cone size $R \equiv \sqrt{(\Delta\eta)^2 + (\Delta\phi)^2}$.

For each event we identify and store indices of the following objects present in the HEPG bank: partons from initial state radiation (ISR), propagator radiation, top quarks, top quark final state radiation (FSR) or t-FSR, W bosons, bottom quarks, hadronic W daughters, FSR emitted from b quarks, FSR emitted from the W daughters and "visible" leptons from W decay. We impose a requirement that all forms of radiated partons have $E_T > 3.0$ GeV (otherwise they are ignored). This transverse energy cut is imposed since partons that do not pass it mimic the energy flow from the underlying event and therefore it would not make sense to give any special consideration to those partons.

2.2 Jet to parton matching

The events are grouped into separate categories based on the jet-to-parton matching of the daughters of the hadronically decaying W boson. It is important to provide a clear description of the algorithm used in order to properly understand the results:

- For each jet in the collection given, all partons from the classes mentioned above are considered. If a parton lies within R units from the current jet position, the index of this parton is stored. Thus at the end of this step for every jet we have a collection of partons close to this jet.
- For the parton of interest we iterate through the jet collection and store the indices of the jets that lie within R of that parton.
-
  - If there are no jet indices accummulated in the previous step we assign a category "0" to this parton.

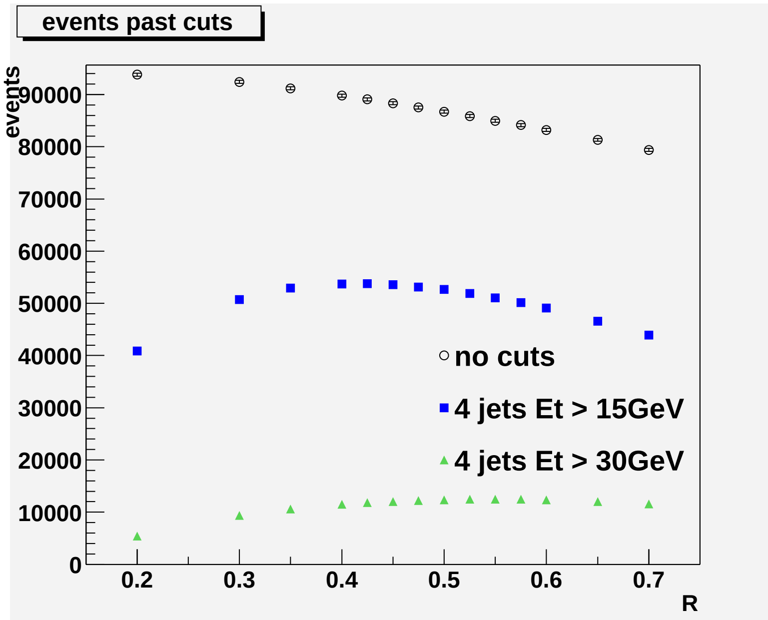

Figure 1: The number of events passing all cuts.

- If there is exactly one jet index accumulated and the jet at this position in the collection has no other partons within the cone size used in the jet clustering, we say that the jet is uniquely matched. This class of partons gets the label "1".
- If there is only one jet index stored for the parton but the jet at this position has one or more partons within R in addition to the parton of interest, than the parton is labelled as "2."
- If there is more than one jet index stored for the parton, it implies that there are at least two jets close to this parton. Such partons are assigned the label "3".

The parameter R used here is always the same as the cone size parameter used by the JetCluModule.

2.3 Event Selection

If the visible lepton from the W boson decay is an electron, we require that there is a uniquely matched jet to this electron. Note that the JetClu algorithm is not responsible for lepton identification; therefore the calorimetry signal caused by an electron will be clustered to form a jet object. If there is no jet uniquely matched to the electron this event will not be included in the analysis. On the other hand if such a "jet" can be found we remove it from the jet collection. If the lepton is a muon, we do not remove any jets from the collection. Cuts based on raw jet transverse energies will be applied to this reduced jet collection. We haven't attempted to apply the lepton selection criteria typical of a lepton + jet event sample as we believe that the jet resolution and reconstruction efficiency largely factorize. The number of events passing the cuts is dependent on the cone size used. This is shown in Fig. 1.

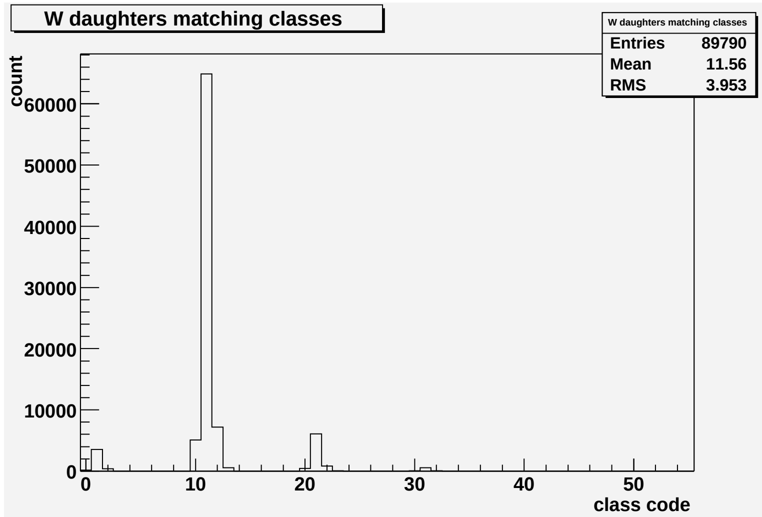

Figure 2: The distribution of the primary event "matching class" based on the jet-to-parton matching of W boson daughters. See the text for a description of each class.

2.4 Event classification

Primary event classification is based on the (hadronically decaying) W boson daughter's matching class. We code each event with the class $10c_1 + c_2$, where c_1 and c_2 are the matching category for the first and second W boson daughter (as found in the HEPG bank). The distribution of these event classifications is shown in Fig. 2 for $R = 0.4$. Note that in the case of W boson daughters the jet-to-parton matching is performed as outlined above in Sec. 2.2, with the exception that FSR emitted from W boson daughters is not considered as a parton close to the jet in the first step of the algorithm. This is done to prevent the categorization of partons that emit FSR into the cone as not uniquely matched (category 2 partons). However, we take into account the possibility of FSR emitted from the complementary W boson daughter flowing into the jet associated with the other daughter.

For each jet we determine if FSR associated with a particular W boson daughter lies within the cone size. If the jet is also associated with the complementary W daughter than that daughter will be classified as "2". The most desirable class of events corresponds to the bar labeled "11". In this case both W daughters are uniquely matched to jets. The invariant mass obtained from the matching jets is shown in the Fig. 3 for the case where $R = 0.4$.

We also classify the events based on the b quark-to-jet matching in a similar way. The jet to parton algorithm described earlier is also applied here. The possibility of a b quark emitting FSR into the cone belonging to the other b quark is handled in the same way as in the case of FSR emitted from complementary W boson daughters. Note that those categorizations are independent. In both cases the matching radius is always the same as the JetClu cone size R.

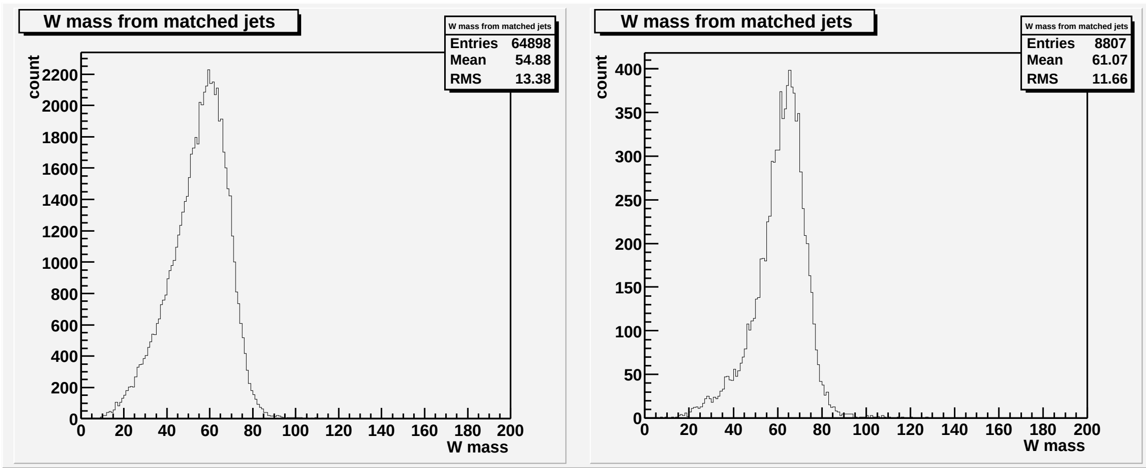

Figure 3: The invariant mass distribution of the dijet system when the W boson daughters fall into the "11" class. The distribution on the left is for events with no jet E_T cuts. The distribution on the right is for events with at least 4 jets with $E_T > 30\ GeV$. A cone size of $R = 0.4$ has been employed.

3 W Boson Mass Resolution

We performed our matching studies for a range of clustering radii from $R = 0.2$ to $R = 0.7$ and for three different sets of kinematic cuts on the observed jets. For each value of R the central region of the W mass distribution is iteratively fitted to a Gaussian distribution, as described below. Figure 4 shows the means of those distributions as a function of R with

- no cuts applied,
- requiring ≥ 4 jets with $E_T \geq 15$ GeV, and
- requiring ≥ 4 jets with $E_T \geq 30$ GeV.

Cuts are applied based on the uncorrected jet energies. As expected, the mean of the reconstructed invariant mass distribution rises as a function of R since more energy gets clustered into the jet as the cone size increases. Upon applying the kinematic cuts, the means are increased by several percent but the overall behaviour doesn't change.

One of the measures of W mass resolution is the standard deviation, σ, of a fit to the "core" of the invariant mass distribution. The behaviour of σ is shown in Fig. 5 as a function of the jet clustering cone size. The resolution drops by 4-6% when the cone size is varied from 0.4 to 0.5 for samples with no kinematic selection and with the 15 GeV jet cuts are imposed. When the 30 GeV jet cut is imposed the variation of the standard deviation with growing cone size is not as strong.

We note that the fitted value of σ is a function of the region chosen for the invariant mass fit. Our fitting procedure is the same for all the points. A fit is first performed on the entire region of the W invariant mass plot. We then iterate the fit twice, each time defining the fit region as extending $\pm 1\ \sigma$ from the mean of the distribution, where those parameters are obtained from the previous iteration. Since the W mass distribution is non-Gaussian, a

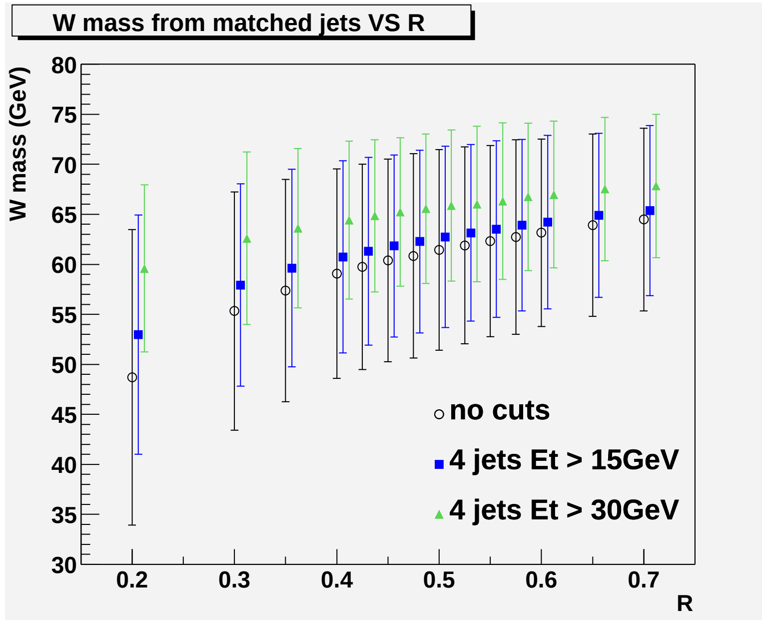

Figure 4: Mean of the W boson mass distribution.

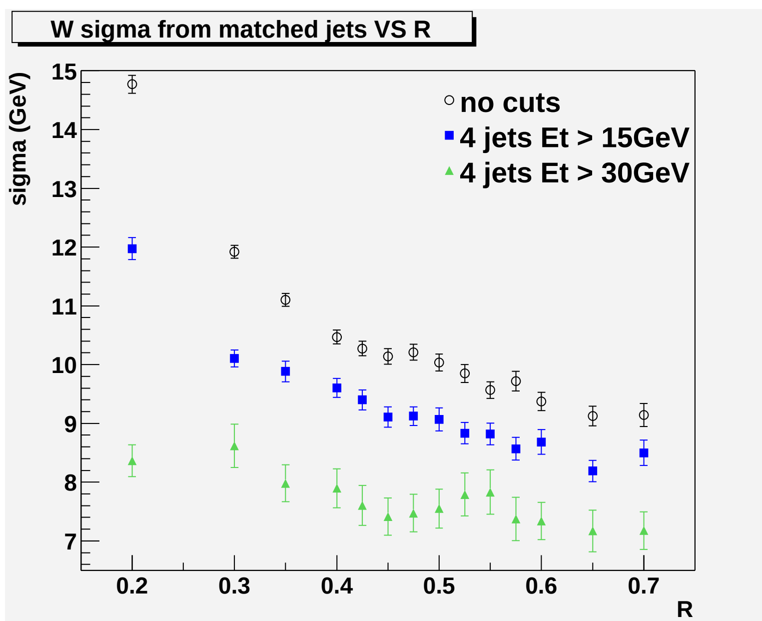

Figure 5: The standard deviation of the W boson mass distribution.

different choice of fitting procedure will produce slightly different results, but this provides a consistent relative measure of the invariant mass resolution as we vary JETCLU cone size and event selection requirements.

A simpler and perhaps equally informative measure of the W mass resolution is the raw root-mean-sqare (RMS) of the W boson mass distribution, as illustrated in Fig. 6. The RMS decreases fairly uniformly over the entire range of cone radii for all cuts. In particular,

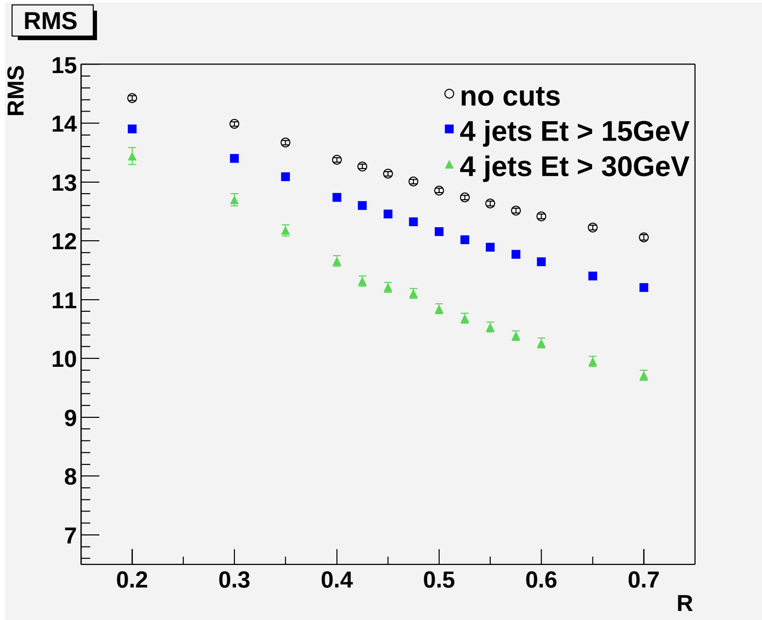

Figure 6: The RMS width of the invariant mass distribution for the dijet system as a function of cone size.

the RMS is reduced by approximately 4% (no cuts or 15 GeV jet cuts) to approximately 7% for 30 GeV jet cuts when the cone radius is increased from 0.4 to 0.5. Generally it is expected that this behaviour would occur. As the cone size is increased, less energy is radiated outside of the cone, improving the jet energy measurement. In addition, as more stringent cuts are applied the RMS values shift down by a constant. This behaviour is caused by the change in the shape of the W mass distribution (cf. Fig. 3), with the tail at lower invariant masses being reduced as the more stringent kinematic cuts are applied.

4 Reconstruction Efficiency

Unfortunately, we pay a price for increasing the cone size. Large cone sizes allow for multiple partons to be clustered into the same cone. This is well illustrated by Fig. 7, where we plot the fraction of events in which at least one W daughter has been ambiguously matched with another parton to a jet. As one can see, the count of partons labeled as "2" – not uniquely matched – increases with the cone size. One of the more interesting quantities one can measure, when trying to minimize the W mass uncertainty, is the fraction of events for which both W daughters are matched to a jet uniquely. The evolution of this quantity as a function of R for all kinematic cuts is shown in Fig. 8. In all cases this fraction is maximized for R=0.3. It is expected that for extremely small cone sizes this fraction will vanish, since a small cone will begin to compete with the intrinsic angular resolution for a jet. As the cone radius increases from 0.4 to 0.5, the fraction of events with both W daughters uniquely matched decreases by approximately 10%. Requiring $\geq$ 4 jets with $E_T \geq 15$ GeV raises this fraction in this region of R by approximately 5%. However, requiring more stringent cuts does not affect the measurement appreciably.

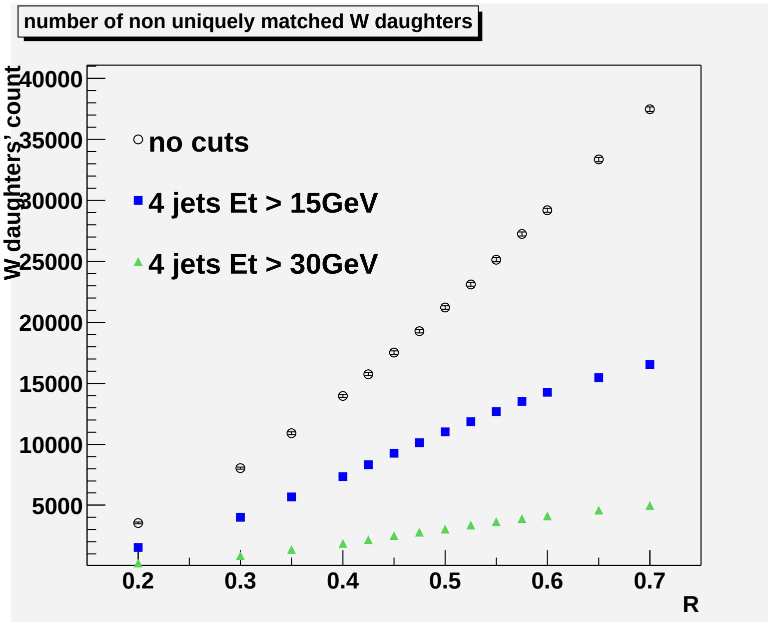

Figure 7: The number of W bosons where at least one of the daughters is ambiguously identified with another parton in the event as a function of jet clustering cone size.

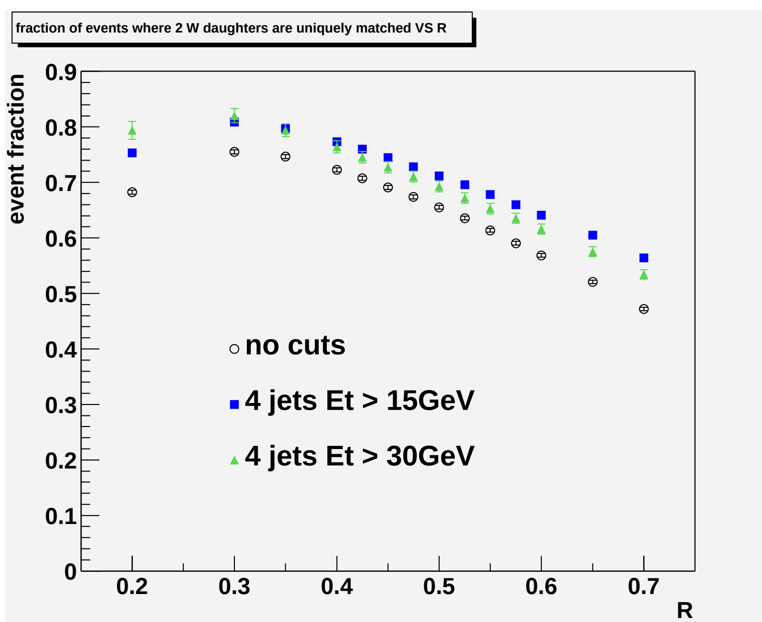

Figure 8: The fraction of events where both W daughters are uniquely matched.

Accurate measurement of the top mass depends on our ability to match both W boson daughters and b quarks to jets. We have therefore plotted the fraction of events where exactly 2, 3 or 4 partons from the direct top quark daughter partons (b, $\bar{b}$, q, $\bar{q}'$) are uniquely matched in Fig. 9.

The most desirable outcome is when all four partons are matched. This is maximized

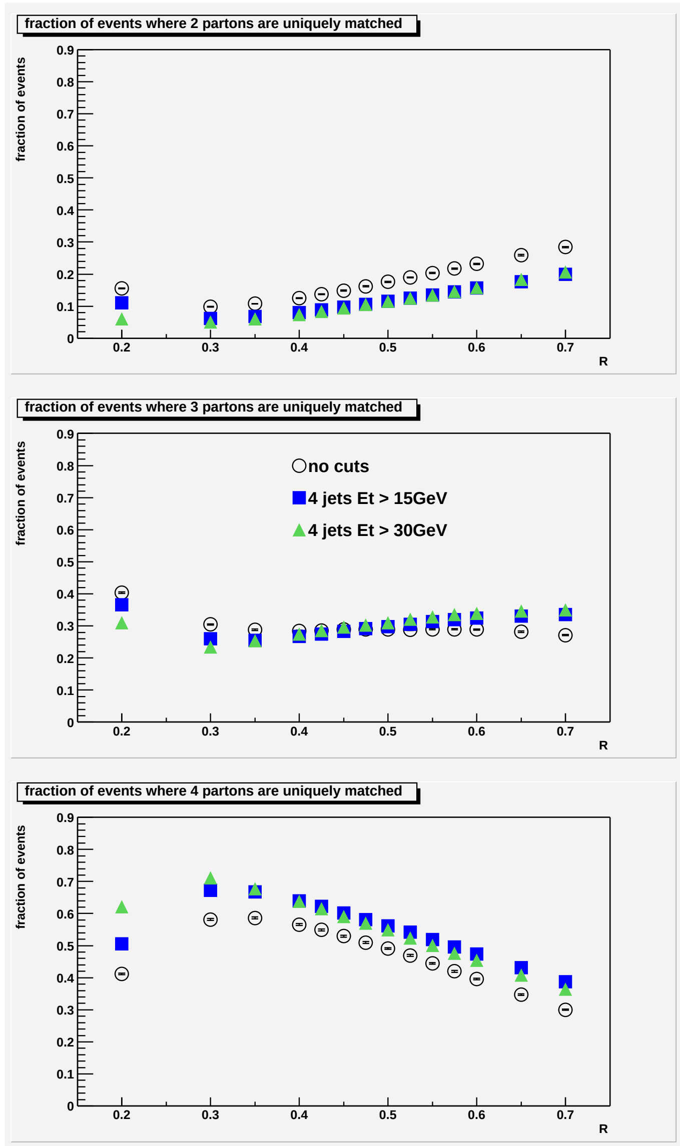

Figure 9: The rate of matching of 2, 3 and 4 partons in $t\bar{t}$ events as a function of jet clustering cone size.

for $R = 0.35$ or 0.3 depending on the choice of jet E_T cuts. When the jet cone size R is increased from 0.4 to 0.5, the fraction of such events decreases by $(13.2 \pm 0.6)\%$ when no cuts are imposed, by $(12.1 \pm 0.7)\%$ when we require ≥ 4 jets with $E_T \geq 15$ GeV and and by $(13.8 \pm 1.4)\%$ when we require ≥ 4 jets with $E_T \geq 30$ GeV. Imposing the most restrictive cuts does not improve the ratio of events with all partons uniquely matched. When no cuts are applied, the approximately constant value of the fraction of events with 3 partons matched suggests that we lose events from the "all parton matched" class to the "3 partons matched" class at the same rate that we lose events from the latter class to the "2 partons matched" class. This is indeed the case: We lose $(7.5 \pm 0.3)\%$ of all events over the region of R from 0.4 to 0.5 in the "all partons matched" class, but we gain $(5.0 \pm 0.2)\%$ of all events in the "2 partons matched" class. When the cuts are imposed it is evident that events are

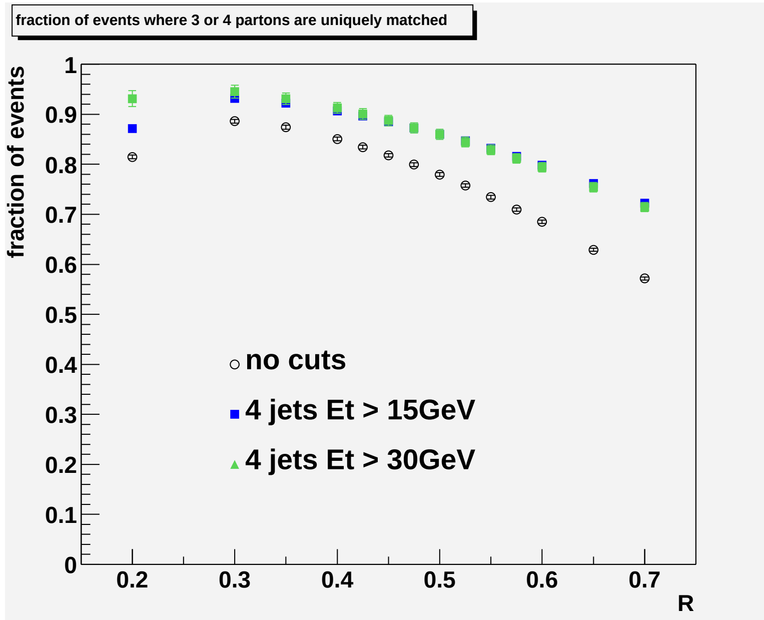

Figure 10: The rate of matching of three or more partons in $t\bar{t}$ events as a function of jet clustering cone size.

lost at higher rate from the "all matched" class to "3 matched" class than from that class to the classes with fewer matched partons.

The fraction of events where 3 or more partons are uniquely matched is shown in Fig. 10. This cumulative fraction is maximized for $R = 0.3$ for all choice of jet E_T cuts. When the R value varies from 0.4 to 0.5, the matching fraction decreases by $(8.3 \pm 0.5)\%$, $(5.2 \pm 0.6)\%$ and $(5.8 \pm 1.3)\%$ when there are no cuts imposed, 15 GeV jet cuts imposed and 30 GeV jet cuts imposed, respectively. There appears to be little benefit in applying cuts beyond 15 GeV.

5 Discussion

We have attempted to classify the sources of non-unique matching in the case of the W decay daughters. This is simplified by the fact that in the case of a non-unique match there is only one other parton flowing into the jet cone 70-80% of the time (Fig. 11). This allows for identifying the most important effects just by studying the case when only one other parton flows into the jet cone.

Most frequently it is the ISR that is causing non-unique matching. This is shown in Fig 12. The effects of ISR on the W mass resolution have been studied earlier [4].

The other very important effect that causes non-unique matching is the b quark lying within the cone of the W daughter (Fig. 13). For low transverse energy cuts on the jets, this effect when considered together with the effect of FSR emitted by the b quark is even more important than one mentioned above. When b quark and W daughter jets are merged the calorimeter signal is not separable into parts corresponding to either parton based on

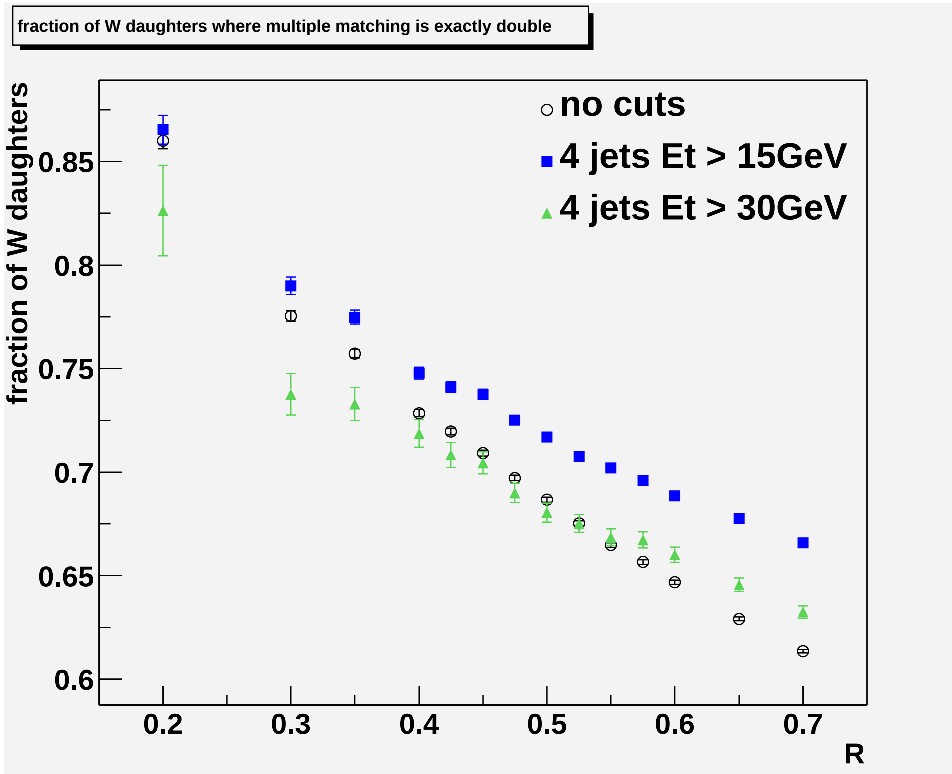

Figure 11: Fraction of the non-uniquely matched W daughters where only one more parton flows into non-uniquely matched W daughter jet.

calorimetry information alone.

We have considered the possibility of the two jets caused by W daughters merging. The relative importance of this effect and the importance of the FSR emitted by one W daughter flowing into the cone of the complementary daughter is quite modest, as shown in Fig. 14. The low importance of these effects can be understood through Fig. 15. This shows the separation of the W daughters in $\eta\phi$ space versus the transverse momentum of the W boson (these are generator-level quantities for all $t\bar{t}$ events). One sees that the W daughters remain well separated till the W boson P_T exceeds approximately 130 GeV/c.

6 Conclusions

We summarize our observations in the following way:

1. Steady improvement in W boson mass resolution as R increases, although most of the benefit comes from a reduction in the RMS of the distribution as opposed to the shrinkage of its "core." For values of $R > 0.5$, we do not observe an appreciable reduction in σ.

2. Unique matching is maximized for surprisingly small values of R in between 0.3 and 0.4. The same is true when we attempt to maximize the rate of unique matching of all four $t\bar{t}$ daughter jets.

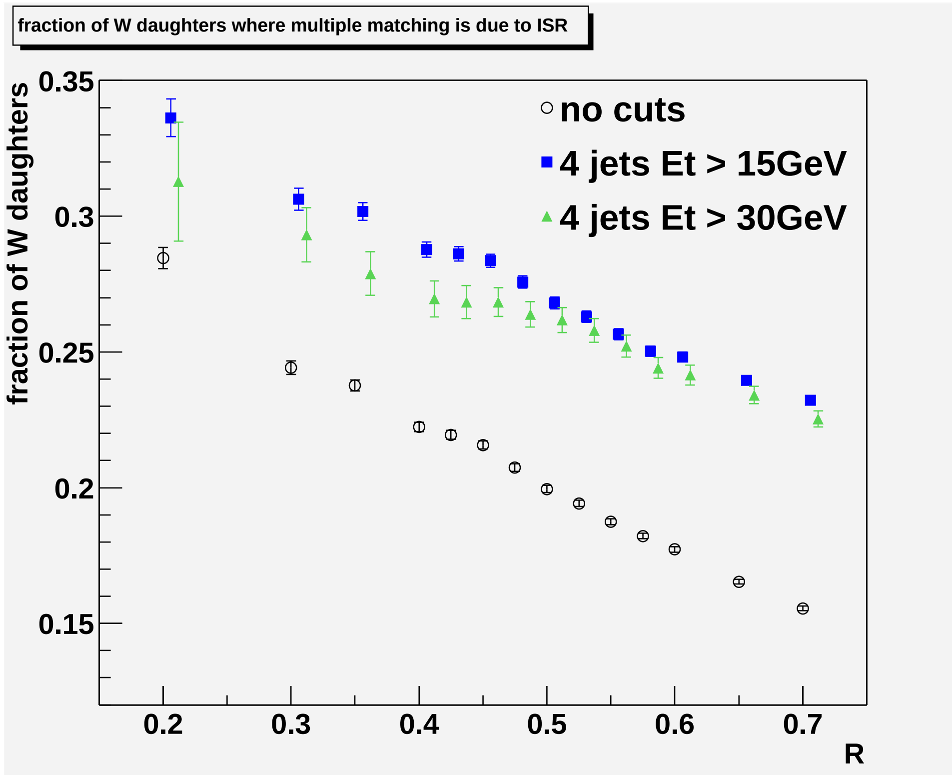

Figure 12: Fraction of the non-uniquely matched W daughters where non-unique matching is due to ISR.

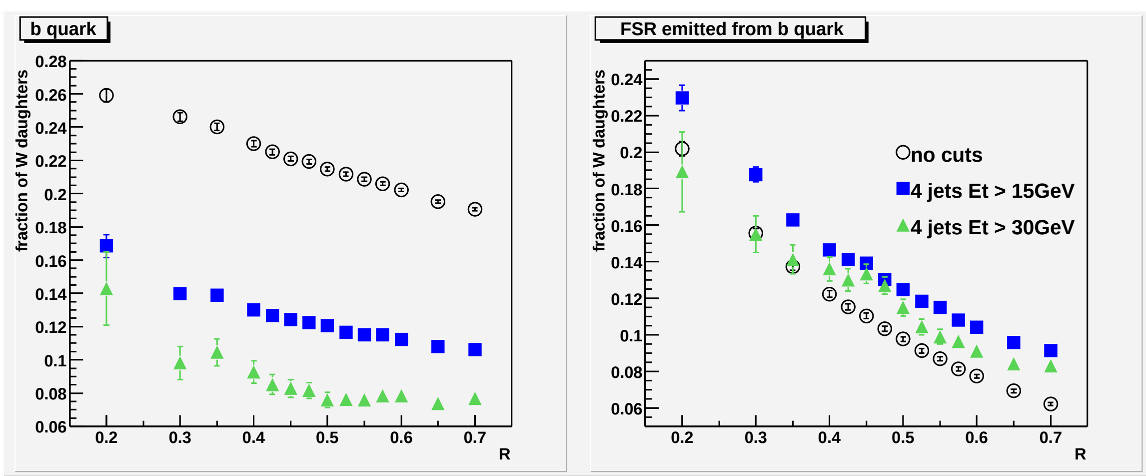

Figure 13: Fraction of the non-uniquely matched W boson daughters where non-unique matching is due to b quark (left) and FSR emitted by the b quark.(right)

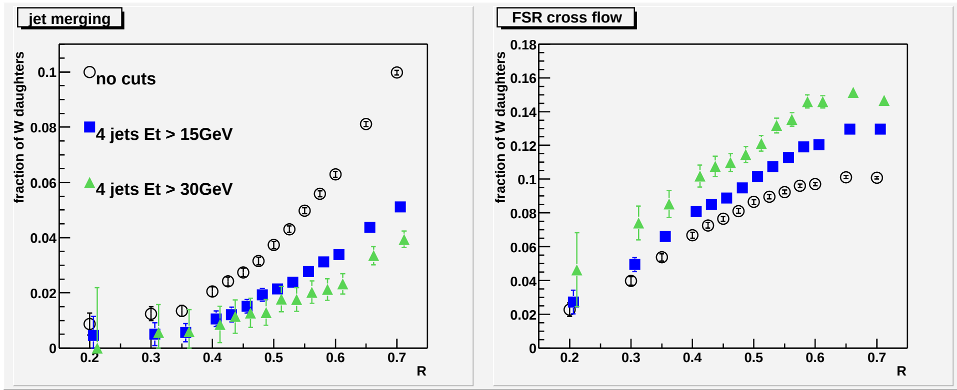

Figure 14: Fraction of the non-uniquely matched W daughters where non-unique matching is due to the W daughters' jets merging (left) and FSR cross-flow between the two jets (right).

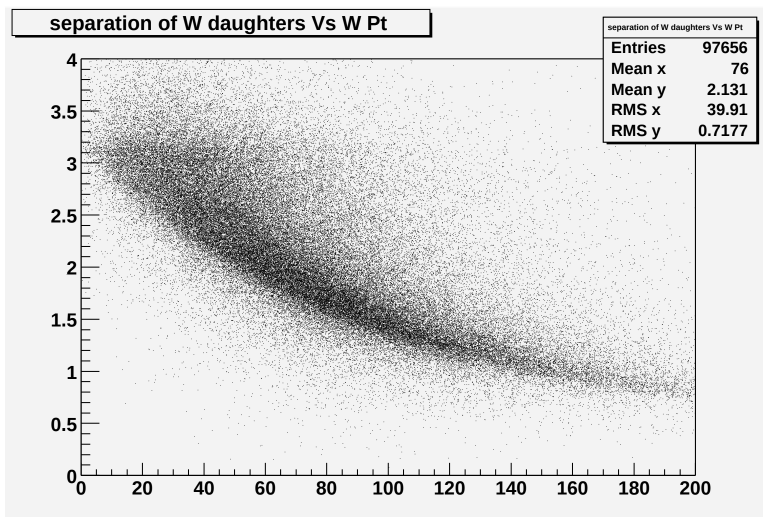

Figure 15: The $\eta - \phi$ separation of W daughters versus the W boson P_T (all $t\bar{t}$ events at the generator level).

3. Ambiguous matching arises primarily from initial state radiation (ISR). For example, for $R = 0.5$, 24% of the ambiguous matches fome from ISR, 11% of them come from confusion with b quark fragments, about 12% come from confusion with b quark FSR, about 8% comes from FSR from the complementary W daughter and only 2% comes from the W daughter itself.

For convenience some of the results are presented in the Table 1.

Overall, these observations suggest that reconstruction of $t\bar{t}$ daughter jets using a simple cone algorithm with cone size $R = 0.5$ is not likely to be optimal, either for maximizing the efficiency of jet-tagging OR for maximizing the event-to-event resolution. This conclusion has to be tempered by the fact that we have ignored a significant effect in our study, namely the combinatorial confusion caused by parton-misassignments. However, our study does suggest that we may gain significantly by using a smaller cone size for jet counting

R	N	mean	RMS	q,q' both matched	4 partons	3 or 4 partons
no E_T cuts on jets						
0.3	92409	55.3 ± 11.9	13.99 ± 0.04	$(75.5 \pm 0.4)\%$	$(58.2 \pm 0.3)\%$	$(88.6 \pm 0.4)\%$
0.35	91184	57.4 ± 11.1	13.67 ± 0.04	$(74.6 \pm 0.4)\%$	$(58.6 \pm 0.3)\%$	$(87.4 \pm 0.4)\%$
0.4	89790	59.1 ± 10.5	13.38 ± 0.04	$(72.3 \pm 0.4)\%$	$(56.6 \pm 0.3)\%$	$(85.1 \pm 0.4)\%$
0.45	88330	60.4 ± 10.1	13.14 ± 0.04	$(69.1 \pm 0.4)\%$	$(52.9 \pm 0.3)\%$	$(81.8 \pm 0.4)\%$
0.5	86706	61.4 ± 10.0	12.85 ± 0.04	$(65.5 \pm 0.4)\%$	$(49.1 \pm 0.3)\%$	$(78.0 \pm 0.4)\%$
0.55	84959	62.3 ± 10.0	12.63 ± 0.04	$(61.4 \pm 0.4)\%$	$(44.5 \pm 0.3)\%$	$(73.4 \pm 0.3)\%$
0.6	83200	63.2 ± 9.4	12.42 ± 0.04	$(56.8 \pm 0.3)\%$	$(39.6 \pm 0.3)\%$	$(68.5 \pm 0.3)\%$
0.65	81313	63.9 ± 9.1	12.23 ± 0.04	$(52.1 \pm 0.3)\%$	$(34.7 \pm 0.2)\%$	$(62.9 \pm 0.3)\%$
0.7	79375	64.5 ± 9.1	12.06 ± 0.04	$(47.2 \pm 0.3)\%$	$(30.0 \pm 0.2)\%$	$(57.2 \pm 0.3)\%$
4 jets with $E_T \geq 15$ GeV reqired						
0.3	50736	57.9 ± 10.1	13.40 ± 0.05	$(80.9 \pm 0.5)\%$	$(67.2 \pm 0.5)\%$	$(93.2 \pm 0.5)\%$
0.35	52899	59.6 ± 9.9	13.09 ± 0.05	$(79.7 \pm 0.5)\%$	$(66.7 \pm 0.5)\%$	$(92.2 \pm 0.5)\%$
0.4	53720	60.7 ± 9.6	12.74 ± 0.04	$(77.4 \pm 0.5)\%$	$(63.9 \pm 0.4)\%$	$(90.7 \pm 0.5)\%$
0.45	53552	61.8 ± 9.1	12.46 ± 0.04	$(74.4 \pm 0.5)\%$	$(60.1 \pm 0.4)\%$	$(88.5 \pm 0.5)\%$
0.5	52667	62.7 ± 9.1	12.16 ± 0.04	$(71.2 \pm 0.5)\%$	$(56.2 \pm 0.4)\%$	$(86.0 \pm 0.5)\%$
0.55	51041	63.5 ± 8.8	11.89 ± 0.05	$(67.8 \pm 0.5)\%$	$(51.9 \pm 0.4)\%$	$(83.2 \pm 0.5)\%$
0.6	49101	64.2 ± 8.7	11.64 ± 0.05	$(64.1 \pm 0.5)\%$	$(47.4 \pm 0.4)\%$	$(79.8 \pm 0.5)\%$
0.65	46590	64.9 ± 8.2	11.40 ± 0.05	$(60.5 \pm 0.5)\%$	$(43.1 \pm 0.4)\%$	$(76.2 \pm 0.5)\%$
0.7	43927	65.4 ± 8.5	11.20 ± 0.05	$(56.4 \pm 0.4)\%$	$(38.8 \pm 0.3)\%$	$(72.2 \pm 0.5)\%$
4 jets with $E_T \geq 30$ GeV reqired						
0.3	9386	62.6 ± 8.6	12.70 ± 0.10	$(82.0 \pm 1.3)\%$	$(71.1 \pm 1.1)\%$	$(94.5 \pm 1.3)\%$
0.35	10621	63.6 ± 8.0	12.18 ± 0.09	$(79.4 \pm 1.2)\%$	$(67.8 \pm 1.0)\%$	$(93.1 \pm 1.2)\%$
0.4	11524	64.4 ± 7.9	11.66 ± 0.09	$(76.4 \pm 1.1)\%$	$(63.8 \pm 1.0)\%$	$(91.3 \pm 1.1)\%$
0.45	12059	65.2 ± 7.4	11.21 ± 0.08	$(72.7 \pm 1.0)\%$	$(59.2 \pm 0.9)\%$	$(88.8 \pm 1.0)\%$
0.5	12361	65.9 ± 7.6	10.84 ± 0.08	$(69.3 \pm 1.0)\%$	$(55.0 \pm 0.8)\%$	$(86.0 \pm 1.0)\%$
0.55	12471	66.3 ± 7.8	10.53 ± 0.08	$(65.3 \pm 0.9)\%$	$(50.1 \pm 0.8)\%$	$(82.9 \pm 1.0)\%$
0.6	12383	67.0 ± 7.3	10.26 ± 0.08	$(61.6 \pm 0.9)\%$	$(45.5 \pm 0.7)\%$	$(79.4 \pm 0.9)\%$
0.65	12038	67.5 ± 7.2	9.95 ± 0.08	$(57.5 \pm 0.9)\%$	$(40.8 \pm 0.7)\%$	$(75.4 \pm 0.9)\%$
0.7	11583	67.8 ± 7.2	9.71 ± 0.09	$(53.4 \pm 0.8)\%$	$(36.4 \pm 0.7)\%$	$(71.4 \pm 0.9)\%$

Table 1: Summary of results.

and tagging and employ a different measure of the energy of the jets once tagged with this smaller cone that takes into account the unique topologies and kinematics of $t\bar{t}$ production and decay.

References

[1] A number of internal CDF studies have been performed. One of the most recent, for example, is: N. Kuznetsova and R. Roser, "Selecting an Optimal Jet Finding Algorithm for Top Analyses," CDF/PHYS/TOP/PUBLIC/6038 (July 2002).

[2] F. Abe et al. (CDF Collaboration), "Measurement of the Top Quark Mass with the Collider Detector at Fermilab," Phys. Rev. D **63**, 032003 (2001).

[3] G. Corcella et al., “An Event Generator for Hadron Emission Reactions with Interfering Gluons,” hep-ph/0011363. We used version 6.202.

[4] A. Robson, “W Mass Resolution at CDF,” senior thesis (December 1999).